Eur. Phys. J. A (2021) 57:251
https://doi.org/10.1140/epja/s10050-021-00559-9

THE EUROPEAN PHYSICAL JOURNAL A

Regular Article - Theoretical Physics

Phenomenological investigation of the parton distribution functions (PDFs) and the partonic luminosities in high energy LHC physics

Marzieh Mottaghizadeh, Fatemeh Taghavi-Shahri[a]

Department of Physics, Ferdowsi University of Mashhad, Mashhad, Iran

Received: 3 May 2021 / Accepted: 21 July 2021

Communicated by Rishi Sharma

Abstract The phenomenological investigation of parton distribution functions (PDFs) based on the "valon" model presented here from the QCD ⊗ QED coupled DGLAP evolution equations in the Mellin space. The PDFs are calculated at the next to leading order $\mathcal{O}(\alpha_s^2)$ in QCD, and we consider the QED effects at $\mathcal{O}(\alpha)$; $\mathcal{O}(\alpha\alpha_s)$ and $\mathcal{O}(\alpha^2)$ approximations. We also investigate in detail the phenomenological implications of these PDFs on the partonic luminosities. We conclude that at the region of the large values for the di-lepton's invariant mass, the luminosity combinations, quark–quark, quark–antiquark and gluon–gluon, get closer to the luminosity involving photons, suggesting possibly non-negligible phenomenological implications due to the photon channel. We Also done a perfect comparison of our results with those obtained by the NNPDF2.3QED set, NNPDF3.1luxQED set and APFEL and there are a nice agreement between them. We demonstrate the necessity of including QED corrections and photon-induced contributions for a correct determination of the parton distribution functions and partonic luminosities.

1 Introduction

The particle physics programs at the Large Hadron Collider (LHC) achieve to observe processes at an unprecedented level of accuracy, selectivity and experimental sensitivity. As a part of such efforts, to analyses the LHC experimental data, one needs to obtained the theoretical cross-sections for proton–proton interactions and, they are related to the parton distribution functions (PDFs) inside protons at least at the next-to-leading-order (NLO) in QCD which involves $\mathcal{O}(\alpha_s^2)$ corrections. However, at the level of accuracy of LHC, it can be expected that the QED corrections, including those with photon-initiated (PI) processes, can have observable effects as $\mathcal{O}(\alpha)$ at the high scales of energy. Therefore, this issue must be included in the theoretical predictions. In particular, the QED corrections in partonic cross sections should be obtained with corresponding the parton distribution functions produced at NLO and NNLO QCD approximations and the relevant order in QED [1–3]. These results are achieved by modifying the DGLAP [4] factorization scale evolution of the parton distribution functions to include the QED splitting functions. The most important outcome of this change is the necessary incorporation of the photon as a component of the patron densities in the proton.

Recently, several methods have been proposed to solve the coupled DGLAP evolution equations analytically based on the Laplace transform [5,6] and the Mellin transform [7–10]. The MRST2004QED [11] was the first PDF set with both QED corrections and the photon PDF, where the photon PDF was obtained from a model and it tested on HERA data for direct photon production process. Then, the NNPDF2.3QED group [12] was the first group to present a model in which the photon PDF was determined independently based on the Drell–Yan data from LHC. Due to the limited sensitivity of the data used as input in this analysis, the photons PDF affected by large uncertainties. The calculation of the photon PDF from NNPDF2.3QED set was later combined with the state of the quark and gluon PDFs from NNPDF3.0 set, together with a modified QED evolution, to build the NNPDF3.0QED set. The CT group has also released a QED analysis using a similar way with the MRST2004QED one, that named the CT14QED set [13]. In recent years, many efforts have been made to resolve these uncertainties. First, accurate determinations of the photon distribution function at the input have been performed and developed by using experimental data related to the elastic form factors of the proton. More accurately, the photon PDF corresponds to the

[a] e-mail: taghavishahri@um.ac.ir (corresponding author)

Published online: 05 August 2021

flux of the emitted photons, and the contribution of the elastic and inelastic emission of the photon PDF is directly related to the corresponding structure functions investigated in the lepton–proton scattering [14,15]. The idea has been modified in different works [16,17] and has been demonstrated in a theoretical framework by the LUXqed group [18,19], where they were the first group to make a publicly available photon PDF to using this approach. Recently, the PDF set including the photon PDF which is based on the LUXqed approach has been generated by the NNPDF group [20].The MMHT group [21,22] consider the effects of QED in their evolution too. They obtained the photon PDF, $\gamma(x, Q^2)$, based on the similar method with those from LUXQED group. They take into account their lower starting scale of energy for the evolution than the LUXQED group.

The main purpose of this paper is to calculate the parton distribution functions and the partonic luminosities in the valon model. The valon model is a phenomenological model originally proposed by Hwa [23]. In this model, the recombination of partons into hadrons occurs in two steps: in the first step, the quarks emit and then absorb the gluons (photons), and become a quark–gluon (photon) cloud that becomes "Valon", then the "Valon" are recombined to hadrons. This model could describe the PDFs, PPDFs, TMDs, and so on, very well [24–28]. In this paper, we analytically investigate the QCD⊗QED coupled DGLAP equations at $\mathcal{O}(\alpha)$, $\mathcal{O}(\alpha\alpha_s)$, $\mathcal{O}(\alpha^2)$ QED and at $\mathcal{O}(\alpha_s^2)$ QCD approximation and obtain PDFs with QED corrections in the valon model. Then we calculate the partonic luminosities and compare them with other available analyses.

The organization of this paper is as follows: in Sect. 2, we present the framework employed to perform our calculations. In this section, we briefly review the valon model for calculating the parton distribution functions with QED corrections and related proton structure functions. Section 3 devoted to the calculation of the parton luminosity distributions which are import issues for analyzing the Drell–Yan processes at the LHC. For this analysis, one needs to know the PDFs with QED corrections. We give our conclusions and outlook in Sect. 4.

2 Review of the PDFs with QED corrections in the valon model

In this section, we present simple parametrization that can be successfully used to determine the PDFs. We consider, besides the $\mathcal{O}(\alpha_s^2)$ QCD corrections, the complete set of $\mathcal{O}(\alpha\alpha_s)$ and $\mathcal{O}(\alpha^2)$ QED corrections to the DGLAP evolution equations. These calculations have been performed in a completely analytically way where we bring out the solutions of these equations in Mellin space [7]. The QCD ⊗ QED DGLAP evolution equations are given as follows,

$$
\begin{aligned}
\frac{\partial q_i(x,Q^2)}{\partial \ln Q^2} &= \sum_{j=1}^{n_f} P_{q_i q_j}(x)\otimes q_j(x,Q^2) \\
&+\sum_{j=1}^{n_f} P_{q_i \bar{q}_j}(x)\otimes \bar{q}_j(x,Q^2) \\
&+P_{q_i g}(x)\otimes g(x,Q^2) \\
&+P_{q_i \gamma}(x)\otimes \gamma(x,Q^2) \\
\frac{\partial \bar{q}_i(x,Q^2)}{\partial \ln Q^2} &= \sum_{j=1}^{n_f} P_{\bar{q}_i q_j}(x)\otimes q_j(x,Q^2) \\
&+\sum_{j=1}^{n_f} P_{\bar{q}_i \bar{q}_j}(x)\otimes \bar{q}_j(x,Q^2) \\
&+P_{\bar{q}_i g}(x)\otimes g(x,Q^2) \\
&+P_{\bar{q}_i \gamma}(x)\otimes \gamma(x,Q^2) \\
\frac{\partial g(x,Q^2)}{\partial \ln Q^2} &= \sum_{j=1}^{n_f} P_{g q_j}(x)\otimes q_j(x,Q^2) \\
&+\sum_{j=1}^{n_f} P_{g \bar{q}_j}(x)\otimes \bar{q}_j(x,Q^2) \\
&+P_{gg}(x)\otimes g(x,Q^2) \\
\frac{\partial \gamma(x,Q^2)}{\partial \ln Q^2} &= \sum_{j=1}^{n_f} P_{\gamma q_j}(x)\otimes q_j(x,Q^2) \\
&+\sum_{j=1}^{n_f} P_{\gamma \bar{q}_j}(x)\otimes \bar{q}_j(x,Q^2) \\
&+P_{\gamma\gamma}(x)\otimes \gamma(x,Q^2)
\end{aligned}
\tag{1}
$$

where n_f is the number of active flavors. The $P_{i,j}$ is the mixed QED and QCD splitting functions in DGLAP evolution equations. It is defined as

$$
\begin{aligned}
P_{ij} &= \alpha_s P_{ij}^{(1,0)} + \alpha_s^2 P_{ij}^{(2,0)} + \alpha P_{ij}^{(0,1)} \\
&+\alpha\alpha_s P_{ij}^{(1,1)} + \alpha^2 P_{ij}^{(0,2)} \\
&i, j \equiv q, \bar{q}, g, \gamma
\end{aligned}
\tag{2}
$$

where the first two terms are related to the pure QCD splitting kernels that write via the usual perturbation expansion and the rest of the terms correspond to the QED, that extracted from theoretical work [29,30]. It is worth to notice that, we don't ignore photon density at high scales of energy, therefore, the momentum sum rule constraint for the partons, modified to include the photon PDF, $\gamma(x, Q^2)$:

$$
\begin{aligned}
&\int_0^1 dx x\Big(\sum_i q_i(x,Q^2) + \bar{q}_i(x,Q^2) \\
&+g(x,Q^2) + \gamma(x,Q^2)\Big) = 1
\end{aligned}
\tag{3}
$$

we have used the new basis of distribution functions and write the coupled and uncoupled evolution equations in Ref. [7]. We analytical solve these evolution equations up to $\mathcal{O}(\alpha_s^2)$ in QCD and $\mathcal{O}(\alpha\alpha_s)$ and $\mathcal{O}(\alpha^2)$ in QED in Mellin space.

The valon model was first proposed by Hwa to investigate the parton distribution functions inside the proton. In this model, proton is a bound state of three "valons". Each valon is a valence quark with its associated sea quarks and glouns. The quantum number of valon is the quantum number of its valence quark and the valons carry all the momentum of proton . In this model, the recombination of parton into hadrons occur in two stage processes: at first, the partons emit and absorb glouns(and here, photon) to evolved the quark–gloun (photon) cloud and became valons. These valons then recombine into hadron. The Fig. 1 shows the schematic picture of the valon model. Therefore, for calculating the parton distribution functions inside proton, we first calculate these PDFs "inside each valon" with initial PDFs at Q_0^2 and using the DGLAP evolution equations. Then, by using the valon distributions inside proton and convolution of these valon distributions with those obtained for PDFs inside valons, we lead to the PDFs in the proton. The motivation for the low value of Q_0^2 is the phenomenological consideration to requires us to choose the initial input densities as $\delta(z-1)$ at Q_0^2 (where, $z=\frac{x}{y}$). This means that at such low initial scale of Q_0^2, the nucleon can be considered as a bound state of three valence quarks which carry all of the nucleon momentum. Therefore, at this scale of Q_0^2, there is one valence quark in each valon and this valence quark carry all of the valon momentum. It is interesting to note that our choice for initial value of Q_0^2 is very close to the transition region reported by the CLAS Collaboration. The first moment of the proton structure function has been measured at CLAS and the results show that there is a transition region around $Q^2 = 0.3\,\mathrm{GeV}^2$ [31]. This choice for Q_0^2 is also close to the initial scale selected by GRSV group which is $Q^2 = 0.4\,\mathrm{GeV}^2$ [32])

In this model, The internal structure of valons at low Q^2 can not be resolved and the valons behave as constituent quarks. The internal structure of valons and the Q^2 dependence of parton distribution functions in the hadron comes from the solutions of the DGLAP evolution equations in each valon with appropriate initial input densities. The valon distribution functions are Q^2 independent. However, they can be denoted as the wave-function square of the constituent quarks in hadron. It also interprets the probability of finding a valon carrying momentum fraction y of hadron momentum. To generate PDFs from the DGLAP evolution equations with QED corrections, one requires these PDFs at some starting scale, $Q_0^2 = 0.283\,\mathrm{GeV}^2$, from which the PDFs may be evolved to higher scales. Now we can calculate the parton distribution functions with QED corrections in the proton:

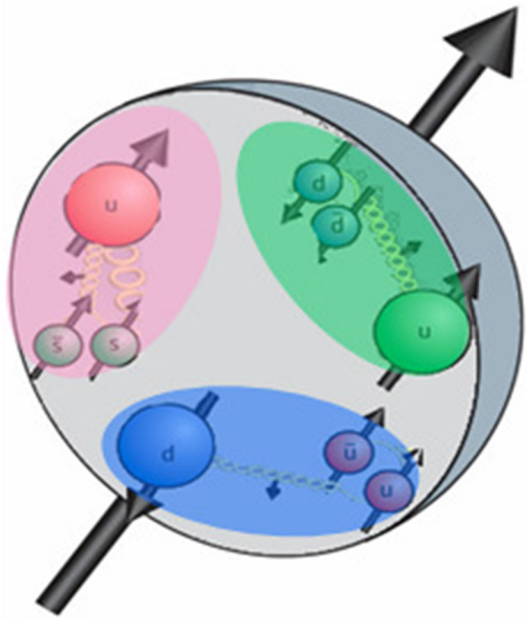

Fig. 1 The schematic picture of the valon model

$$q^p(x,Q^2) = \sum_{valon} \int_x^1 dy G^p_{\mathrm{valon}}(y) q^{\mathrm{valon}}\left(\frac{x}{y}, Q^2\right) \tag{4}$$

where $G^p_{\mathrm{valon}}(y)$ is the distribution of the valon with momentum fraction y in the proton. The valon distribution functions given by the following expressions [23,33–35],

$$G_{U/p}(y) = \frac{B(\alpha+1,\beta+1)y^{\alpha}(1-y)^{\alpha+\beta+1}}{B(\alpha+1,\beta+1)B(\alpha+1,\alpha+\beta+2)} \tag{5}$$

$$G_{D/p}(y) = \frac{B(\alpha+1,\alpha+1)y^{\beta}(1-y)^{2\alpha+1}}{B(\alpha+1,\beta+1)B(\alpha+1,\alpha+\beta+2)} \tag{6}$$

where $B(m,n)$ is the Beta function and $\alpha = 1.545$ and $\beta = 0.89$ [23,33–35].

The determination of parton content of proton requires the knowledge of the valon distribution inside proton. Let us denote the probability of finding a valon carrying momentum fraction y of the proton by $G_{valon/p}(y)$, which describes the wave function of proton in the valon representation, containing all the complications due to confinement. With the requirements that the these equations form satisfies the number and momentum sum rules:

$$\int_0^1 G_{valon/p}(y)dy = 1$$
$$\sum_{valon} \int_0^1 y G_{valon/p}(y)dy = 1 \tag{7}$$

An essential property of the valon model is that the structure of proton in the valon representation is independent of the probe. This means that the parton distribution in a proton can

be written as the convolution of "the partons in the valon" and the "valon distribution in the proton" which are independent of probe or Q^2. The PDFs in the valon, $q^{\text{valon}}(\frac{x}{y}, Q^2)$, conclude from solutions of the DGLAP evolution equations with QED corrections in each valon. The PDFs in a hadron can be written as the convolution of the partons in the valon and the valon distribution function in the hadron. Finally, the PDFs in the proton have the following form

$$
\begin{aligned}
u_{valance}(x, Q^2) &= 2\int_x^1 q_{\frac{valance}{valon}}\left(z=\frac{x}{y}, Q^2\right)G_{U/p}(y)dy \\
d_{valance}(x, Q^2) &= \int_x^1 q_{\frac{valance}{valon}}\left(z=\frac{x}{y}, Q^2\right)G_{D/p}(y)dy \\
\bar{q}_{Sea}(x, Q^2) &= 2\int_x^1 q_{\frac{Sea}{valon}}\left(z=\frac{x}{y}, Q^2\right)G_{U/p}(y)dy \\
&\quad + \int_x^1 q_{\frac{Sea}{valon}}\left(z=\frac{x}{y}, Q^2\right)G_{D/p}(y)dy \\
g(x, Q^2) &= 2\int_x^1 q_{\frac{g}{valon}}\left(z=\frac{x}{y}, Q^2\right)G_{U/p}(y)dy \\
&\quad + \int_x^1 q_{\frac{g}{valon}}\left(z=\frac{x}{y}, Q^2\right)G_{D/p}(y)dy \\
\gamma(x, Q^2) &= 2\int_x^1 q_{\frac{\gamma}{valon}}\left(z=\frac{x}{y}, Q^2\right)G_{U/p}(y)dy \\
&\quad + \int_x^1 q_{\frac{\gamma}{valon}}\left(z=\frac{x}{y}, Q^2\right)G_{D/p}(y)dy \quad (8)
\end{aligned}
$$

where $\bar{q}_{Sea}(x, Q^2)$ is the total distribution of all sea quarks. In this analysis, we consider five active flavors, and also $\Lambda_{QCD} = 0.22\,\text{GeV}$. In this model, we can calculate the total distribution of all sea quarks. Here, we know how can separate the different kind of sea quarks distributions when we have the total distribution of all sea quarks. In this paper, we consider $\bar{u} = \bar{d}, s = \bar{s}, c = \bar{c}$ and $b = \bar{b}$. We have studied the symmetry breaking of sea quarks distribution functions, and we have used the fact that probability of finding heavier partons inside proton are smaller than those of light partons. We have mentioned this in detail in Ref. [9].

The parton distribution functions at different values of Q^2 are shown in Fig. 1. It is clear that increasing Q^2 leads to a decrease in the valance quark distributions (Fig. 2). Furthermore, the contribution of the photon distribution function are increased with increasing the value of Q^2. It means that the photon distribution function is significant at high scales of Q^2.

In order to validate the efficiency and emphasize the phenomenological impact of this method, the reduced cross-section are presented and discussed. In the following, we present a detailed comparison of the theoretical predictions based on the valon model for reduced cross-section in terms of DIS structure functions. The common variables in any DIS process are as follows: the photon virtuality $Q^2 = -q^2$, where q is the difference of the four-momenta; the longitudinal momentum fraction $x = Q^2/2qP$, where P is the four-momentum of the incoming proton; and the inelasticity $y = Q^2/sx$, where s is the center of mass energy squared determined from the electron and proton beam energies. The reduced cross-section is given by

$$
\sigma_r = F_2(x, Q^2) - \frac{y^2}{1+(1-y)^2}F_L(x, Q^2)\ , \quad (9)
$$

Then, σ_r is determined by two structure functions, $F_2(x, Q^2)$ and $F_L(x, Q^2)$. These DIS structure functions are proportional with PDFs. In Fig. 3, we present the theory predictions based on the valon model for the reduced cross-section, σ_r, as a function of x, Q^2 at center of mass energy of $\sqrt{318}\,\text{GeV}$ for different values of Q^2. The model predictions for σ_r are then compared with experimental data from HERA (H1 experiment). The results show a nice agreement between them.

3 The partonic luminosities

In this section, we discuss the effect of higher and mixed orders of $\mathcal{O}(\alpha\alpha_s)$, and $\mathcal{O}(\alpha^2)$ QED corrections on the evolution of PDFs and its impact on the luminosity at the present center of mass energies available at the LHC. To calculate the cross-sections in hadron collision processes, the PDF contributions factorize in the form of the parton luminosities. In a similar way to the DIS structure functions for electron–proton collisions, the production cross sections in proton–proton collisions can be factorized in terms of the convolution between two universal PDFs and a process-dependent partonic cross section. In full generality, for the case of the total inclusive cross section for a narrow resonance production with mass M, the cross section can be factorized as

$$
\sigma = \sum_{i,j=q,\bar{q},g}\int_{M^2}^{s}\frac{ds}{s}\mathcal{L}_{ij}(s, \mu^2)s\hat{\sigma}_{ij}(s, M^2, \mu^2) \quad (10)
$$

where s is the squared centre of mass energy of the two incoming partons. The usefulness of this factorized form above equation is that the complete PDF dependence of the hadronic cross section is now encoded in the partonic luminosities $\mathcal{L}_{ij}$. Therefore, at a hadron collider, all factorizable observable for the production of a final state with invariant mass of M

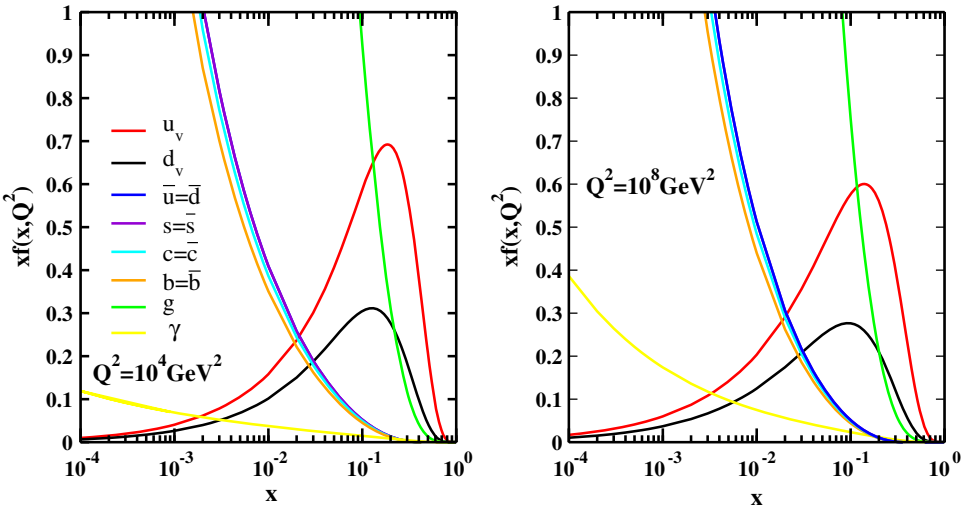

Fig. 2 The parton distribution functions as a function of x at two values of $Q^2 = 10^4\,\text{GeV}^2$ and $Q^2 = 10^8\,\text{GeV}^2$

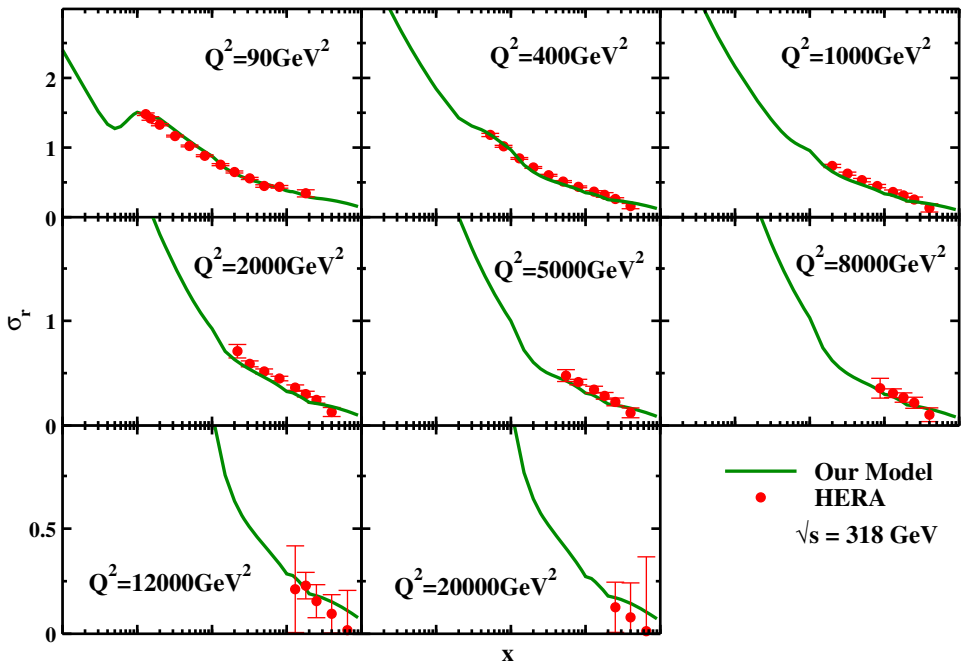

Fig. 3 The comparison of reduced cross-sections as a function of x and Q^2 at center of mass energy of $\sqrt{318}\,\text{GeV}$ for different values of Q^2 with those from experimental data

depend on the parton distribution functions through a parton luminosity. Then, before looking at specific processes, it is a good idea to study the behavior of the parton luminosities of the different initial state. In the following, we explain how we can obtain the partonic luminosity distribution for proton–proton collisions at the different center of mass energies. The results obtaied for PDFs with QED corrections in previous section help us to calculate these luminosities at the LHC energies. The luminosity distribution $dL_{ij}/dlnM^2$ for partons i and j in proton–proton collisions is defined by [18],

$$\frac{dL_{ij}}{dlnM^2} = \frac{M^2}{s}\int \frac{dz}{z} f_i(z, M^2) f_j\left(\frac{M^2}{zs}, M^2\right) \tag{11}$$

where s is the squared center of mass energy of the hadronic collision, and M is the invariant mass. In Eq. (11), $f_i(x; M^2)$ is the PDF of the ith parton evaluated at the factorization scale $Q = M$. To improve predictions from a particular process, this distribution can be adopted different choices for Q. At the level of pure luminosities, without the convolution with any specific matrix element, the factorization scale can be naturally set to $Q = M$. We used the PDFs obtained in the previous section to calculate the luminosity distributions. In Fig. 4, we show the gluon–gluon luminosity as a function of invariant mass M for four center of mass energies 8, 13, 33, and 100 TeV, with the factorization scale Q set equal to M. We also compare them with those from APFEL, NNPDF3.1luxQED, and NNPDF2.3QED global analysis [12,18–20]. This figure shows that for the entire range in M considered at the four different proton–proton collision energies, gluon–gluon luminosities are compatible with these analyses.

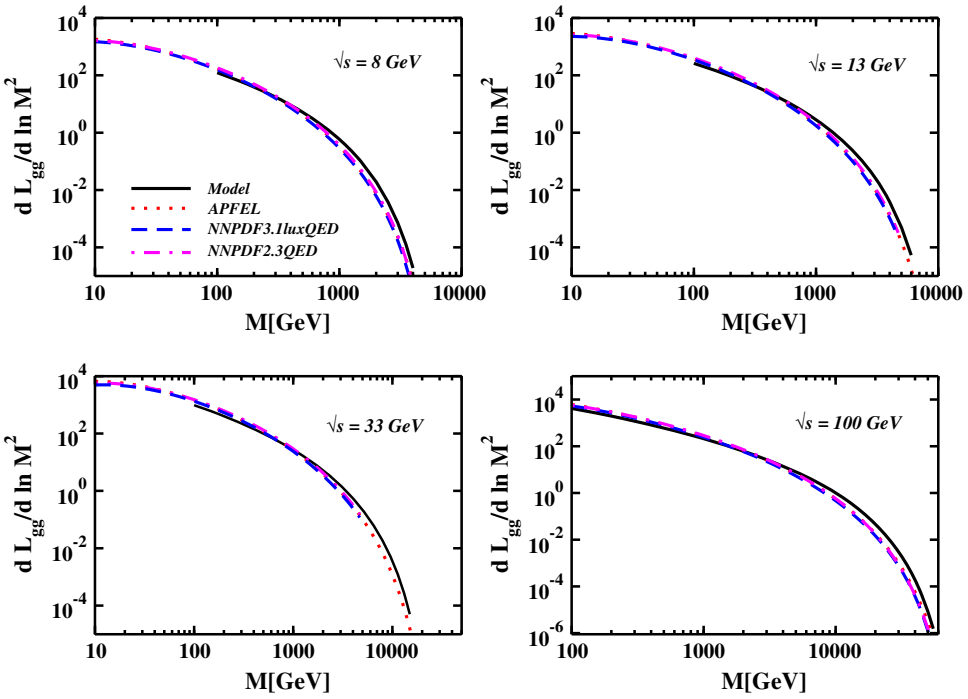

Fig. 4 The gg luminosity distributions in pp collisions, as a function of the partonic invariant mass M, at center of mass energies of 8 TeV, 13 TeV, 33 TeV and 100 TeV

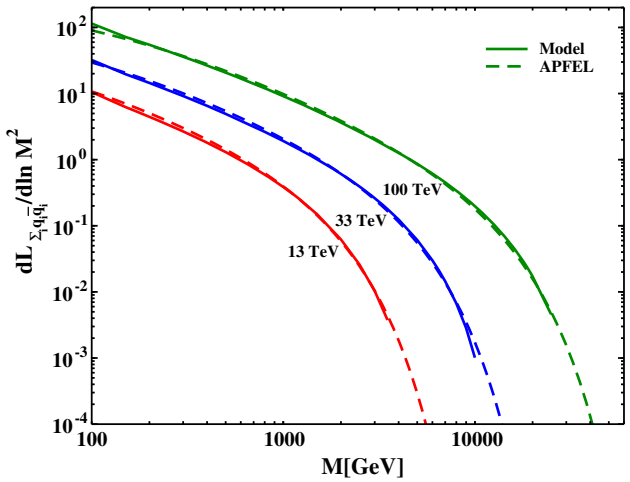

Fig. 5 The $\sum_i q_i \bar{q}_i$ luminosity distributions in pp collisions, as a function of the partonic invariant mass M, at center of mass energies of 13 TeV, 33 TeV and 100 TeV

For the $\sum_i q_i \bar{q}_i$ luminosity distribution, we have included a factor of two in the sum, since either quarks or antiquarks can come from each beam. In Fig. 5, we show quark–antiquark luminosity distribution for our model at $\sqrt{s}$ =13, 33 and 100 TeV. We compare them with the results extracted from APFEL. The plot shows there is a good agreement between them.

In Fig. 6, we depicted the quark–quark luminosity distributions, $dL_{uu}/dlnM^2$ and $dL_{dd}/dlnM^2$ and compare them with those from APFEL at $\sqrt{s}$ =13, 33 and 100 TeV. The $\gamma\gamma$ partonic luminosity is shown in Fig. 7, as a function of the $\gamma\gamma$ invariant mass of M, for several center of mass energies. The $\gamma\gamma$ luminosity is about three orders of magnitude smaller than the gluon–gluon, quark–quark, and quark–antiquark luminosities over a wide range of invariant masses.

The Fig. 7 shows differences between the results predicted by the valon model and those obtained by APFEL for $\gamma\gamma$ partonic luminosities. These differences mainly concern the initial scale of energy, Q_0. As we mentioned in Sect. 2 the initial photon PDF, $\gamma(x, Q^2)$, is equal to zero at $Q_0^2 = 0.283\,\mathrm{GeV}^2$. The practical implementation of the DGLAP evolution equations from the initial scale Q_0 to the scale Q would also lead to the additional differences.

Therefore, the PDF sets are based on a completely different assumption for $\gamma(x, Q^2)$ at the initial scale of Q_0. The MRST2004QED and CT14QED sets, the functional form define for the photon PDF at the initial scale of Q_0, is assumed to be completely determined by the valence quark distributions. The photon parametrization at the initial scale of Q_0 is defined by

$$f_{\gamma/p}(x, Q_0) = \frac{\alpha}{2\pi} (A_u e_u^2 \tilde{P}_{\gamma q} \otimes u^0(x) + A_d e_d^2 \tilde{P}_{\gamma q} \otimes d^0(x)) \quad (12)$$

In the NNPDF2.3QED, NNPDF3.0QED, and NNPDF3.1lux QED sets no functional form is specified for the photon distribution function at the initial scale. The photon distribution function is only constrained to be positive. In the first step, the PDF replicas for all the partons are fit together from DIS data only. Afterwards, they are further constrained by Drell-Yan data form the LHC Run-I at 7 TeV [13].

It is important to note that the behavior of the photon PDF at small x and large Q, the region where the differ-

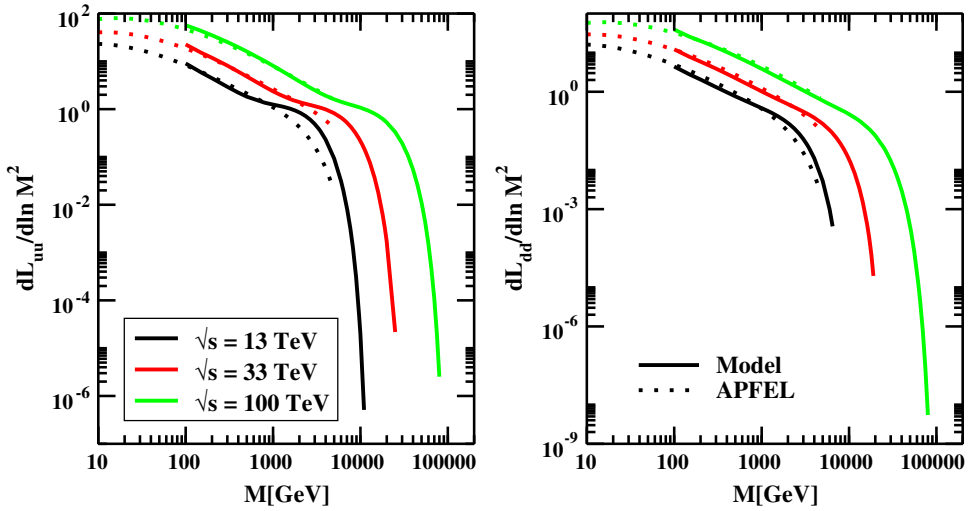

Fig. 6 The uu and dd luminosity distributions in pp collisions as a function of the $\gamma\gamma$ invariant mass M, for collider center of mass energies of 13 TeV, 33 TeV and 100 TeV

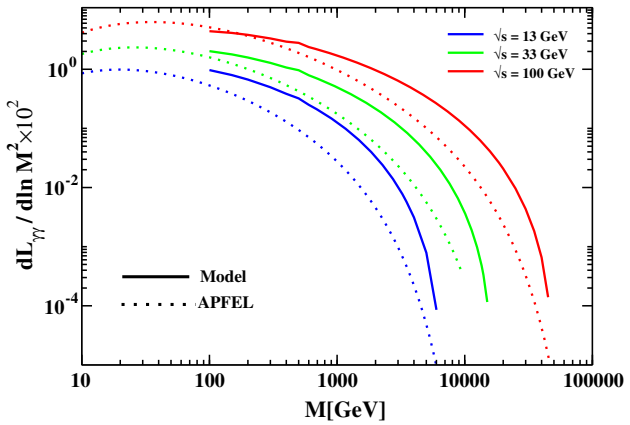

Fig. 7 $\gamma\gamma$ partonic luminosity distributions as a function of $\gamma\gamma$ invariant mass at center of mass energies of 8, 13, 33 and 100 TeV

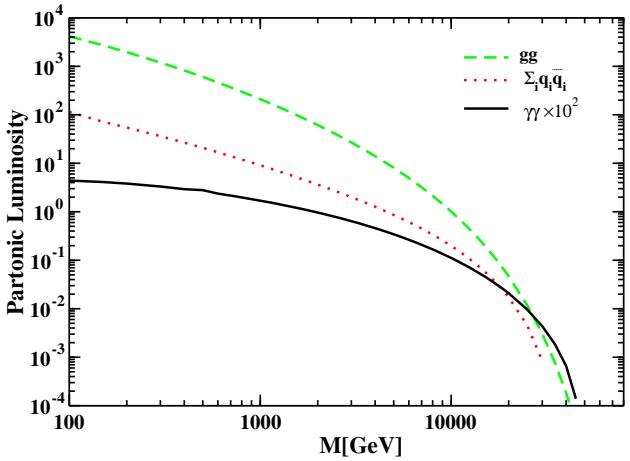

Fig. 8 The comparison of partonic luminosities as a function of $\gamma\gamma$ invariant mass at center of mass energy of 100 TeV

ences among the PDF sets are large and are determined by the QCD ⊗ QED DGLAP evolution equations. Moreover, at small values of M, where small values of x can be probed, the quarks and gluons PDFs are much larger than the photon PDF, leading to a relative suppression of photon-initiated contributions. As previously observed in Fig. 7, the inclusion of these higher-order splitting functions in the evolution of $x\gamma(x, Q^2)$ tend to reduce its magnitude, particularly at the higher range in x. It is noted that near TeV scales, the importance of these higher orders becomes significant, concluding a $\mathcal{O}(5\%)$ reduction in the total $\gamma\gamma$ luminosity.

These figures show that for the high invariant mass of M region that this value related to the value of the center of mass energy, the luminosity combinations, quark–quark, quark–antiquark, and gluon–gluon, get closer to the luminosities involving photons that suggesting possibly non-negligible phenomenological implications due to photon channel. The major part of this effect is caused by the relative behavior of the strong coupling α_s with respect to the QED coupling α as functions of the scale M. As is well known, DGLAP evolution leads to an increase of PDFs in the small-x region and to a decrease in the large-x region as the evolution scale increases. The magnitude of such a behavior is driven by the rate of change of the coupling, no matter whether it is negative, as for α_s, or positive, as for α. Given that the absolute value of the QCD β-function is larger than the QED one up to very large scales, α_s-driven PDFs, like quark and gluon PDFs, are relatively more suppressed at larger values of x as compared to α-driven PDFs, like photon PDFs. To show this, we compare the gluon–gluon, $\sum_i q_i\bar{q}_i$ and $\gamma\gamma$ luminosities at center of mass energy $\sqrt{s} = 100\,TeV$ in Fig. 8. It is obvious from Eq. (11) that the behavior of the M-differential luminosities at large values of invariant mass M reflects the behavior of PDFs at large values of x and thus, according to the argument above, QCD luminosities are more repressed than QED luminosities in this region and finally they get overtaken.

4 Conclusions and outlook

In this paper, we have presented the updated parton distribution functions, modified to include the effects of QED in their evolution. The procedure developed to provide an approximate QED at $\mathcal{O}(\alpha)$, $\mathcal{O}(\alpha\alpha_s)$, $\mathcal{O}(\alpha^2)$ corrections to the DGLAP evolution equations, is the valon model. We have done all steps in the Mellin space. Finally, we have obtained the photon–photon, gluon–gluon, quark–quark and quark–antiquark luminosities at the various colliders center of mass energies and compared them with the results from NNPDF2.3QED set, LUXqed set, and APFEL. We have arrived at a good agreement between them. We found that the QCD luminosity combinations, quark–quark, quark–antiquark and gluon–gluon, get closer to the luminosities involving photons for the region of high invariant mass M. The behavior of the M-differential luminosities at the large values of invariant mass M reflects the behavior of parton distribution functions at large values of x and thus, the QCD luminosities are more suppressed than QED luminosities in this region and finally they get overcome. High-precision experimental measurements of W and Z production at the LHC on the percent level, as well as future measurements at the high-luminosity LHC or future high-energy colliders such as FCC (Future Circular Collider), will demand equally precise resumed predictions in QCD⊗QED evolution.

Acknowledgements This work is supported by the Ferdowsi University of Mashhad under Grant number 73209(25/12/1397).

Data Availability Statement This manuscript has no associated data or the data will not be deposited. [Authors' comment: There is no data in the paper because all experimental data used in this analysis is properly cited and referred to.]

References

1. R.D. Ball et al., [NNPDF Collaboration], arXiv:1706.00428 [hep-ph]
2. R.D. Ball et al., [NNPDF Collaboration], JHEP **1504**, 040 (2015). https://doi.org/10.1007/JHEP04(2015)040. arXiv:1410.8849 [hep-ph]
3. A.D. Martin, W.J. Stirling, R.S. Thorne, G. Watt, Eur. Phys. J. C **63**, 189 (2009). https://doi.org/10.1140/epjc/s10052-009-1072-5. arXiv:0901.0002 [hep-ph]
4. S. Carrazza, arXiv:1509.00209 [hep-ph]
5. M. Mottaghizadeh, P. Eslami, F. Taghavi-Shahri, Int. J. Mod. Phys. A **32**(14), 1750065 (2017). https://doi.org/10.1142/S0217751X17500658. arXiv:1607.07754 [hep-ph]
6. M. Zarei, F. Taghavi-Shahri, S.A. Tehrani, M. Sarbishei, Phys. Rev. D **92**(7), 074046 (2015). https://doi.org/10.1103/PhysRevD.92.074046. arXiv:1601.02815 [hep-ph]
7. M. Mottaghizadeh, F.T. Shahri, P. Eslami, Phys. Lett. B **773**, 375 (2017). https://doi.org/10.1016/j.physletb.2017.08.049. arXiv:1707.00108 [hep-ph]
8. M. Mottaghizadeh, A. Mirjalili, Nucl. Phys. A **993**, 121643 (2020). https://doi.org/10.1016/j.nuclphysa.2019.121643
9. M. Mottaghizadeh, F.T. Shahri, P. Eslami, Phys. Rev. D **96**(7), 074001 (2017). https://doi.org/10.1103/PhysRevD.96.074001. arXiv:1707.00845 [hep-ph]
10. S. Moch, J.A.M. Vermaseren, A. Vogt, Nucl. Phys. B **688**, 101 (2004). https://doi.org/10.1016/j.nuclphysb.2004.03.030. arXiv:hep-ph/0403192
11. A.D. Martin, R.G. Roberts, W.J. Stirling, R.S. Thorne, Eur. Phys. J. C **39**, 155 (2005). https://doi.org/10.1140/epjc/s2004-02088-7. arXiv:hep-ph/0411040
12. R.D. Ball et al., NNPDF Collaboration, Nucl. Phys. B **877**, 290 (2013). https://doi.org/10.1016/j.nuclphysb.2013.10.010. arXiv:1308.0598 [hep-ph]
13. C. Schmidt, J. Pumplin, D. Stump, C.P. Yuan, Phys. Rev. D **93**(11), 114015 (2016). https://doi.org/10.1103/PhysRevD.93.114015. arXiv:1509.02905 [hep-ph]
14. L. Harland-Lang, V. Khoze, M. Ryskin, Eur. Phys. J. C **76**(5), 255 (2016). https://doi.org/10.1140/epjc/s10052-016-4100-2. arXiv:1601.03772 [hep-ph]
15. A. Mukherjee, C. Pisano, Eur. Phys. J. C **30**, 477–486 (2003). https://doi.org/10.1140/epjc/s2003-01308-0. arXiv:hep-ph/0306275
16. J. Blumlein, G. Levman, H. Spiesberger, J. Phys. G **19**, 1695–1703 (1993). https://doi.org/10.1088/0954-3899/19/10/029
17. M. Łuszczak, W. Schöfer, A. Szczurek, Phys. Rev. D **93**(7), 074018 (2016). https://doi.org/10.1103/PhysRevD.93.074018. arXiv:1510.00294 [hep-ph]
18. A. Manohar, P. Nason, G.P. Salam, G. Zanderighi, Phys. Rev. Lett. **117**(24), 242002 (2016). https://doi.org/10.1103/PhysRevLett.117.242002. arXiv:1607.04266 [hep-ph]
19. A.V. Manohar, P. Nason, G.P. Salam, G. Zanderighi, JHEP **1712**, 046 (2017). https://doi.org/10.1007/JHEP12(2017)046. arXiv:1708.01256 [hep-ph]
20. V. Bertone, S. Carrazza, J. Rojo, Comput. Phys. Commun. **185**, 1647 (2014). https://doi.org/10.1016/j.cpc.2014.03.007. arXiv:1310.1394 [hep-ph]
21. L.A. Harland-Lang, A.D. Martin, R. Nathvani, R.S. Thorne, Eur. Phys. J. C **79**(10), 811 (2019). https://doi.org/10.1140/epjc/s10052-019-7296-0. arXiv:1907.02750 [hep-ph]
22. R. Nathvani, R. Thorne, L. Harland-Lang, A. Martin, PoS DIS **2018**, 029 (2018). https://doi.org/10.22323/1.316.0029. arXiv:1807.07846 [hep-ph]
23. R.C. Hwa, Phys. Rev. D **22**, 759 (1980). https://doi.org/10.1103/PhysRevD.22.759
24. F. Taghavi-Shahri, Z.A. Yazdi, S.A. Tehrani, Int. J. Theor. Phys. **58**(1), 157–166 (2019). https://doi.org/10.1007/s10773-018-3920-2
25. J. Sheibani, A. Mirjalili, S.A. Tehrani, Int. J. Theor. Phys. **59**(5), 1553–1571 (2020). https://doi.org/10.1007/s10773-020-04423-2
26. Z.A. Yazdi, F. Taghavi-Shahri, F. Arash, M.E. Zomorrodian, Phys. Rev. C **89**(5), 055201 (2014). https://doi.org/10.1103/PhysRevC.89.055201. arXiv:1401.1295 [hep-ph]
27. F. Arash, Phys. Rev. D **50**, 1946–1950 (1994). https://doi.org/10.1103/PhysRevD.50.1946
28. G.R. Boroun, M. Amiri, Phys. Scr. **88**, 035102 (2013). https://doi.org/10.1088/0031-8949/88/03/035102. arXiv:1402.0162 [hep-ph]
29. D. de Florian, G.F.R. Sborlini, G. Rodrigo, Eur. Phys. J. C **76**(5), 282 (2016). https://doi.org/10.1140/epjc/s10052-016-4131-8. arXiv:1512.00612 [hep-ph]
30. D. de Florian, G.F.R. Sborlini, G. Rodrigo, JHEP **1610**, 056 (2016). https://doi.org/10.1007/JHEP10(2016)056. arXiv:1606.02887 [hep-ph]
31. R. Fatemi et al., CLAS Collaboration, Phys. Rev. Lett. **91**, 222002 (2003). https://doi.org/10.1103/PhysRevLett.91.222002. arXiv:nucl-ex/0306019

32. M. Gluck, E. Reya, M. Stratmann, W. Vogelsang, Phys. Rev. D **63**, 094005 (2001). https://doi.org/10.1103/PhysRevD.63.094005. arXiv:hep-ph/0011215
33. R.C. Hwa, Phys. Rev. D **51**, 85 (1995). https://doi.org/10.1103/PhysRevD.51.85
34. R.C. Hwa, C.B. Yang, Phys. Rev. C **66**, 025205 (2002). https://doi.org/10.1103/PhysRevC.66.025205. arXiv:hep-ph/0204289
35. R.C. Hwa, C.B. Yang, Phys. Rev. C **66**, 025204 (2002). https://doi.org/10.1103/PhysRevC.66.025204. arXiv:hep-ph/0202140